



Contents lists available at <http://qu.edu.iq>

Al-Qadisiyah Journal for Engineering Sciences

Journal homepage: <https://qjes.qu.edu.iq/>



# Application of LES/PDF and RANS/PDF approaches for simulation of spray combustion

Duaa Y. Haran\* and Ahmed A. Majhool

Department of mechanical engineering, University of Al-Qadisiyah, Al-Qadisiyah, Iraq.

## ARTICLE INFO

### Article history:

Received 14 April 2021

Received in revised form 6 May 2021

Accepted 13 June 2021

### Keywords:

Spray combustion

Eulerian/Lagrangian

Turbulence model

Fluent

## ABSTRACT

This paper is addressing of a coupling Large-eddy simulation (LES) and RANS turbulence models with mixture fraction/probability density function as a combustion model. The two models have been implemented to simulate ethanol-air spray combustion. The gas phase is described with the Eulerian approach while the liquid phase is designed using a Lagrangian framework. The LES/PDF approach is obtained statistically. The sub-grid scale energy equation is used with the LES/PDF approach. The numerical results are validated with experimental data. Both LES/PDF and RANS/PDF approaches are compared with the experimental data. The LES/PDF approach shows good agreement in predicting the average gas temperature compared with RANS/PDF approach. The LES/PDF shows a better prediction of both turbulence intensity profiles and the vortices which are generated in the turbulent flow in comparison with the RANS/PDF approach.

© 2021 University of Al-Qadisiyah. All rights reserved.

## 1. Introduction

Liquid fuels are widely used in industrial combustion systems like the internal combustion engine, liquid-fueled rockets, and gas turbines. It plays a significant role in our energy supply. Typically, liquid fuels are provided as a turbulent spray into the combustion chamber. The efficiency of combustion, stability, and pollutant formation depend heavily on the turbulent spray characteristics [1-6]. Therefore, attention must be paid to understanding the mechanism of turbulent spray combustion and developing methods that would give a clearer picture of the behavior of such phenomena. Modeling and numerical simulation are considered challenging because it involves complex processing such as turbulence, phase change, heat transfer, and chemical reactions. In recent years, large-eddy simulation of liquid spray combustion has received a lot of attention. LES can provide more accurate statistical results and detailed dynamic flow

and flame structures compared to Reynolds-averaged modeling (RANS). In the future, it is predicted that the LES turbulence model will become a widely used computational fluid dynamics method that will replace RANS modeling [7, 8]. There are many pieces of research in LES on turbulent two-phase flow and liquid spray combustion that were reviewed by the current authors. Jones et al. [9] CFD simulation of swirl stabilized flames fueled by liquid kerosene were provided by large-eddy simulation (LES). There were two flames studied for which experimental data was available. Flame (A) was a stable flame, while flame (B) was unstable due to its lower air-fuel ratio. The results of a combined LES/PDF technique were applied to high swirl reacting spray flows and compared to empirical data. The formulation took into account sub-grid turbulence-spray-chemistry interactions, as well as the coupling between the gas and liquid phase.

\* Corresponding author.

E-mail address: [mech.post04@qu.edu.iq](mailto:mech.post04@qu.edu.iq) (Duaa Y.haran)



Dodoulas et al. [10] Three pre-mixed piloted turbulence CH<sub>4</sub>/air flames at different Reynolds numbers were subjected to Large-eddy simulation/Filtered Density Function model. In contrast to experimental data using the same closures used in non-premixed combustion with no changes to the combustion regime, the results showed strong agreement. The effect of heat release on the flow domain was investigated and correctly captured. The results showed that pre-mixed combustion could be modeled using LES/PDF methods, at least under work conditions, and that approach could reliably capture spray conditions where combustion was not significant and large pockets of extinction emerged. Heye et al. [11] The experimental data of a pilot-established ethanol spray flame were analyzed using the LES/ODF method. A Lagrangian Monte-Carlo model was used to solve the PDF equation. The droplet evaporation occurred way from the flame front, separating the two processes. Owing to the high flow rate of the droplet-laden air, the front flame was unable to propagate. As compared to the others, there were significant differences in the conditions of the droplet inflow. Ukai et al. [12] A combined Large-Eddy Simulation (LES)/Conditional Moment Closure approach applied to model spray combustion. Additional source terms in the transport equation of CMC originating from fuel evaporation were modelled, and their effect on flame structure and global quantities including tentatively averaged temperature profile had been investigated. The laboratory spray jet flame prediction was generally good. The evaporation source term caused a flux in mixture fraction space, which shifted peak temperatures to higher mixture fraction regions. Jones et al. [13] In the GENERIC combustor, LES was used to simulate kerosene/air. The liquid phase was defined using the Eulerian method, which was fully coupled with the Lagrangian method. Reacting and non-reacting environments were simulated in two separate test cases. In terms of mean statistics and flame structure estimation, the flow field simulations were satisfactory. Ukai et al. [14] To model spray combustion, a hybrid Large-Eddy Simulation (LES)/Conditional Moment Closure method was used. The CMC method was coupled with a chemistry table that allowed for spatial and temporal variations of the tabulated chemical composition and provided a fair reliable estimation of the chemical source term of the LES/filtered reaction development variable. The numerical results were validated with experimental of two dilute acetone spray with pre-evaporation. An axial spray velocities and temperature predictions were noticeably enhanced, while RMS velocity showed reasonable agreement. Dodoulas et al. [15] For simulating a non-premixed flame with high extinction, a Large Eddy Simulation/PDF method was used. This method is effective in predicting the local flame extinction at different flame locations, and the major species predictions were found to be in good agreement with the practical data. The flame structure was analyzed by using chemical explosive modes. Due to the turbulence combustion model nature, the statistical data on the sub-grid flame structure can be obtainable. Sub-grid explosive models, for example. According to the results, sub-grid structures were only essential near the inlet nozzle in the current flame, and downstream extinction was controlled by Large-Scale interaction. Wang et al. [16] On the acetone flame structure, three combustion models (finite-rate chemistry model, flame-prolongation of intrinsic low dimensional manifold model, and flamelet-progress variable model) were applied to achieve large-eddy simulation (LES) of a turbulence spray structure. In comparison to experimental results, the use of a finite-rate chemistry model combined with a reduced chemical mechanism results in improved prediction of spray flame structure and heat release among the three models. Sacomano Filho et al. [17] In the form of a C<sub>2</sub>H<sub>5</sub>OH/air turbulence flame, turbulence flame interaction and evaporative cooling effect were investigated in LES turbulence. The artificially thickened flame method

(ATF) was combined with the mixture adaptive thickening extension technique to account for enthalpy variations. The Eulerian/Lagrangian system was used to track the droplets. The flamelet-generated manifold method has been tabulated by chemistry (FMG). Variations in enthalpy were integrated into the outcomes FGM database in a universal manner that was not limited to heat losses due to evaporative cooling effects. Aside from being novel, the proposed modelling strategy's comprehensiveness allowed for a significant contribution to the understanding of turbulent spray combustion modeling's most relevant phenomena. [17] As a result of the introduction of renewable aviation fuels, alternative methods and models are needed that can predict the combustor performance based on the fuel composition. In the sense of Eulerian/Lagrangian the LES, a multi-component vaporization model was coupled with a direct. The burner which used in this work exhibited some of the existing features of aero-engine combustors like the reaction zone position and measured spray combustion were fine reproduced by LES turbulence model. The computational outcomes showed that the evaporation and mixing were the rate-controlling stages in the flame zone. Chemistry can be presumed to be significantly fast in this zone. However, other regions existed where the finite rate chemistry influence available. The approach of the finite rate chemistry demonstrated great potential in terms of pollution formation. Furthermore, the formation of benzene from one specific chemical form in the fuel suggested that to accurately predicted soot emissions, multi-component explanation of the liquid phase and the evaporation process was needed. Paulhiac et al. [18] A spray-swirled burner was subjected to LES/Discrete particle simulation. There are two types of validation: reacting and non-reacting. The velocity field of the two-phase finding was consistent in both cases as compared to experimental data. The LES grid fails to describe the non-premixed flame set near the droplets due to the direct interaction between the spray and flame. Instead, the current model referred to pre-mixed combustion, which allowed for a percentage error in both the burning rate and combustor efficiency. It was necessary for using a single droplet combustion model which is appropriate to the LES/DPS framework. [18] Spray reactive flow is used in a variety of technological instruments. A sub-grid scale combustion model is studied. Two different flamelet methods were implemented which were consisting of spray flamelet and multi-regime gas flamelet models. The numerical evaluation was implemented in large-eddy simulations (LES) of a benchmark C<sub>2</sub>H<sub>5</sub>OH/air spray flame a partial pre-vaporization. An Eulerian/Lagrangian numerical framework was adopted. Outcomes showed that the spray flamelets developed from counterflow partially-premixed spray flames showed a better agreement with the experimental data. In the present work, Ansys Fluent is applied for simulating two-phase flow in 2D, free shear stress with a certain domain 360mm×460 Ge et al. [19]. Large Eddy Simulation (LES) and Reynolds averaged Navier-Stokes equations (RANS) turbulence model are implemented to simulate the turbulent spray of C<sub>2</sub>H<sub>5</sub>OH/air spray. Both turbulence models are combined with a Probability Density Function (PDF) as a combustion model. Then used for investigating using various parameters in an attempt to find out which of approach is the best in giving results closer to the practical results and closer visualization of the practical reality.

## 2. Governing equations

The main physical processes of down-draft evaporative cooling consist of turbulent flow, species mixing, mass, and heat transfer. Differential equations for each species, mass conservation, momentum conservation, and energy conservation must be solved. Also, the transport equations for

the turbulence model should be solved. These equations are employed into three sets, continuous phase (Euler phase) equations used for solving the fluid flow and species transport, dispersed phase (liquid phase ) calculate the trajectory of the fuel droplets, and due to strong cooperation between two-phases, the coupled effect must be solved for the complex environment. All equations and constants used are based on ANSYS Fluent theory Fluent et al. [20]. The general equations that are used for the solution are identified as follows:

### 2.1. Euler phase model

FLUENT ANSYS solves gas-phase flow as well as analysis the differential equations of mass conservation, momentum conservation, energy conservation, and species. In the initial stages of the process, the model solves the gas phase without including the interaction between the two phases, when the liquid phase (disperse particle) trajectories are solved, and the source terms are added [20]. FLUENT solves the gas phase with consideration of the source terms in the numerical calculations. The conservation mass equation is

$$\frac{\partial}{\partial x_i}(\rho u_i) = S_m \quad (1)$$

Where ( $u_i$ ) is the air velocity component in Euler-phase (m/s),  $S_m$  defined as an additional mass to gas-phase from liquid-phase (discrete phase) ( $kg/m^3s$ ). The transformation momentum due to the exchange can be expressed as:

$$\rho u_i \frac{\partial u_i}{\partial x_j} = \frac{\partial}{\partial x_j} \left[ \mu \left( \frac{\partial u_i}{\partial x_j} + \frac{\partial u_j}{\partial x_i} \right) - \frac{2}{3} \mu \left( \frac{\partial u_i}{\partial x_j} \right) \delta_{ij} \right] + \rho g_i - \frac{\partial p}{\partial x_i} + F_i \quad (2)$$

When the species diffusion and the source due to the energy interchange between phases are included, the energy equation is identified in the following part (), where  $S_n$  is the volumetric heat source ( $kg/s^3m$ ), the heat transfer is calculated by using:

$$\rho u_i \frac{\partial e}{\partial x_i} = -P \frac{\partial u_i}{\partial x_i} + \Phi v + \frac{\partial}{\partial x_i} \left( k \frac{\partial T}{\partial x_i} \right) + \frac{\partial}{\partial x_i} (\sum_{i=1}^n h_i J_i) + S_n \quad (3)$$

Where  $\mu$  is the molecular viscosity ( $kg/m^2s^2$ ),  $F_i$  is the momentum source ( $kg/m^2s^2$ ),  $g_i$  is a gravity ( $m/s^2$ ),  $P$  is the static pressure (pa),  $e$  is the internal energy ( $J/kg$ ),  $T$  is the air temperature in ( $K$ ),  $h_i$  is the species enthalpy,  $\Phi v$  is the Rayleigh dissipation function ( $kg/s^3m$ ),  $k$  is the thermal conductivity ( $W/mk$ ),  $J_i$  is the species (i) diffusion flux ( $kg/m^2s$ ). The species conservation equations For predicting the local mass fraction of each phase, i.e., gas-phase of fuel and air, are:

$$\rho u_i \frac{\partial m_i}{\partial x_i} = -P \frac{\partial J_i}{\partial x_i} + S_m \quad (4)$$

$$J_{i=} = -\rho D_{i,m} \frac{\partial m_i}{\partial x_i} \quad (5)$$

Where  $m_i$  is the local mass fraction of specific phase (i) and  $D_{i,m}$  is the diffusion coefficient for a specific phase (i) in the mixture.

### 2.2. Liquid phase model

The discrete droplets in the gas phase are suggested to be spherical. At the start of the solutions, the Lagrangian approach is used to calculate the

trajectory of the particles (discrete phase) by integrating the force balance, while the gas phase is recalculated and adjusted, it solves the liquid phase in the following equations:

$$\frac{dU_p}{dt} = F_D(u - u_p) + \frac{g_x(\rho_p - \rho)}{\rho_p} + \frac{\rho}{\rho_p} u_p \frac{\partial u}{\partial x_i} \quad (6)$$

$$F_D = \frac{18\mu}{\rho_p d_p^2} \frac{C_D Re}{24} \quad (7)$$

$$Re = \frac{d_p \rho |u_p - u|}{\mu} \quad (8)$$

$$C_D = a_1 + \frac{a_2}{Re} + \frac{a_3}{Re^2} \quad (9)$$

where  $u_p$  is the droplets velocity (m/s),  $F_d(u - u_p)$  is the drag force per unit droplet mass ( $m/s^2$ ),  $(g_x(\rho_p - \rho)/\rho_p)$  is the gravitational force on the droplet, the last term on the right hand of the equation represents the additional force due to the pressure gradient in the fuel,  $dU_p/dt$  is the evaporation rate of the droplet,  $g_x$  is the gravity ( $m/s^2$ ),  $C_D$  is the drag coefficient,  $d_p$  is the diameter of the droplet (m), and  $a_1$ ,  $a_2$ , and  $a_3$  are constants obtained by Morsi and Alexander [21]. The heat balance utilizes for computing the heat transfer between the gas phase and the liquid phase. Radiant heat transfer is ignoring, is identified as:

$$m_p c_p \frac{dT_p}{dt} = h_{fg} \frac{dm_p}{dt} + h_p A_p (T_\infty - T_p) \quad (10)$$

where  $A_p$  is the droplet surface area ( $m^2$ ),  $c_p$  is the droplet heat capacity ( $J/kg k$ ),  $T_p$ ,  $T_\infty$  are the temperature of the droplet and gas phase respectively in (k),  $h$  is the convective heat transfer coefficient ( $W/m^2k$ ),  $h_{fg}$  is the latent heat of evaporating fuel ( $J/kg$ ).

### 2.3. Coupling phases

An iterative method is implemented to solve two coupled phases(gas phase and discrete phase). When the computation of the particle stream is done, including the calculation of the gain or loss of mass, momentum, and heat by the particle trajectory, then these quantities are added into the gas-phase (continuous) calculation. The mass exchange between two phases is evaluated as the mass differences between all C.V. using.

$$S_m = \frac{\Delta m_p \dot{m}_{p,o}}{m_{p,o}} \quad (11)$$

where  $S_m$  is the mass exchange,  $\Delta m_p$  is the change of the particle mass in each C.V,  $m_p$  is the particles mass flow rate,  $m_{p,o}$  is the mass flow rate of the particle at the initial state. Then  $S_m$  included in the mass conservation equation. In addition, the gas phase is added as a source of mass in the species equation. The momentum transfer between the two phases can be calculated as:

$$F_{i=} = \sum \left( \frac{18\mu}{\rho_p d_p^2} \frac{C_D Re}{24} (u_p - u) + \frac{g_x(\rho_p - \rho)}{\rho_p} + \frac{\rho}{\rho_p} u_p \frac{\partial u}{\partial x_i} \right) \dot{m}_p \Delta t \quad (12)$$

The vaporization rate of the droplets is controlled by the concentration of the vapor between the surface of the droplet and the gas phase.

$$N_{i=} = k_c (C_{i,s} - C_{i,\infty}) \quad (13)$$

$$K_{c} = \frac{S_h D_{im}}{d_p} = \frac{(2+0.6R_e^{1/2} S_c^{1/3}) D_{im}}{d_p} \quad (14)$$

$$C_{i,\infty} = X_i \frac{P}{RT_\infty} \quad (15)$$

$$C_{i,s} = \frac{P_{sat}(T_p)}{R(T_p)} \quad (16)$$

where  $N_i$  is the vapor molar flux ( $kg\ mole/m^2s$ ),  $K_c$  is the coefficient of the mass transfer ( $m/s$ ),  $C_{i,s}$  is the vapor concentration at the surface of the droplet ( $kg\ mole/m^3$ ),  $C_{i,\infty}$  is the vapor concentration in gas-phase ( $kg\ mole/m^3$ ),  $P_{sat}$  is the vapor pressure at saturated state (pa),  $R$  is the universal gas constant ( $J/kgk$ ),  $S_h$  is the Sherwood number,  $S_c$  is Schmidt number,  $X_i$  is the local bulk mole fraction of specific phase  $i$ . Droplet evaporation is submitted to law 2 in FLUENT, and the change of the droplet mass can be found:

$$m_p(t + \Delta t) = m_p(t) - N_i A_p M_{w,i} \Delta t \quad (17)$$

where  $M_{w,i}$  is the molecular weight of specific phase  $i$  ( $\frac{kg}{mole}$ ),  $S_h$  is the volumetric source term, which can be expressed as

$$S_h = \left[ \frac{\bar{m}_p}{m_{p,o}} c_p \Delta T_p + \frac{\Delta m_p}{m_{p,o}} \left( -h_{fg} + \int_{T_{ref}}^{T_p} C_{p,i} dt \right) \right] \dot{m}_{p,o} \quad (18)$$

where  $\bar{m}_p$  is the droplet average mass in a control volume ( $kg$ )

### 2.3.1. Turbulence model

The turbulence model is a mathematical model used to describe the turbulent flow which is commonly used in a realistic and engineering application. Turbulence models are used to represent turbulence by using simple equations. In this work, standard k- $\epsilon$  and large-eddy simulations are used representing the random and irregular flow.

#### 2.3.1.1. Standard k- $\epsilon$ model

In the Standard model derivation, flow assumes fully turbulent and ignores the influence of molecular viscosity. It is appropriate just for fully turbulent. For the turbulent kinetic energy,  $k$ .

$$\frac{\partial}{\partial t} (\rho k) + \frac{\partial}{\partial x_i} (\rho k u_i) = \frac{\partial}{\partial x_j} \left[ \left( \mu + \frac{\mu_t}{\sigma_k} \right) \frac{\partial k}{\partial x_j} \right] + G_k + G_b - \rho \epsilon - Y_M + S_k \quad (19)$$

For turbulence dissipation rate  $\epsilon$ .

$$\frac{\partial}{\partial t} (\rho \epsilon) + \frac{\partial}{\partial x_i} (\rho \epsilon u_i) = \frac{\partial}{\partial x_j} \left[ \left( \mu + \frac{\mu_t}{\sigma_\epsilon} \right) \frac{\partial \epsilon}{\partial x_j} \right] + C_{1\epsilon} \frac{\epsilon}{k} (G_k + C_{3\epsilon} G_b) - C_{2\epsilon} \rho \frac{\epsilon^2}{k} + S_\epsilon \quad (20)$$

Where  $\mu_t$  is the Turbulent viscosity modeling as :

$$\mu_t = \rho C_\mu \frac{k^2}{\epsilon} \quad (21)$$

$$G_k = -\rho \overline{u_i u_j} \frac{\partial u_j}{\partial x_i} \quad (22)$$

$G_b$  is the effect of buoyancy

$$G_b = \beta g_i \frac{\mu_t}{Pr_t} \frac{\partial T}{\partial x_i} \quad (23)$$

Where the Dissemination rate is  $Y_m$ , the production of turbulent kinetic energy is  $G_k$ , the Turbulent velocity is  $\hat{u}$ , the thermal expansion coefficient is  $\beta$ , the turbulent Prandtl number is  $Pr_t$  is, at default = 0.85, the source term defined by used are  $S_k, S_\epsilon$ , and the reverse active prattle are  $\sigma_\epsilon, \sigma_k$  for  $\epsilon, k$  respectively. Constants model at default value are:

$$C_{1\epsilon} = 1.44, C_{2\epsilon} = 1.92, C_\mu = 0.09, \sigma_k = 1, \sigma_\epsilon = 1.3, C_{3\epsilon} = -0.33$$

#### 2.3.1.2. Sub-grid scale model energy equation stress model

A sub-grid scale equation energy stress model is expressed as:

$$\tau_{ij} = \frac{2}{3} \rho K_{sgs} \delta_{ij} - 2 C_k \rho K_{sgs}^{1/2} \Delta f \overline{S_{ij}} \quad (24)$$

$K_{sgs}$  is acquired by solving the transport equation.

$$\rho \frac{\partial \overline{k_{sgs}}}{\partial t} + \rho \frac{\partial \overline{u_j k_{sgs}}}{\partial x_j} = -\tau_{ij} \frac{\partial \overline{u_i}}{\partial x} - C_\epsilon \rho \frac{K^{3/2}}{\Delta f} + \frac{\partial}{\partial x_j} \left( \frac{\mu_t}{\sigma_k} \frac{\partial K_{sgs}}{\partial x_j} \right) \quad (25)$$

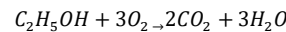
$$K_{sgs} = \frac{1}{2} (\overline{u_k^2} - \overline{u_k}^2) \quad (26)$$

$$\mu_t = C_k \rho K_{sgs}^{1/2} \Delta f \quad (27)$$

$$\Delta f = V^{1/3} \quad (28)$$

Where the filter size is  $\Delta f$ , the sub-grid scale eddy viscosity is  $\mu_t$ .

The mechanism of the reaction is implemented in one step, the ethanol-oxygen reaction is described chemically as:



For the radiative heat transfer, the P1 model is used

$$-\overline{q}_r = aG - 4a\sigma \overline{T}^4 \quad (29)$$

where the Stefan-Boltzmann constant denotes by  $\sigma = 5.67 * 10^{-8} J.K^{-1}$ , the absorption coefficient is  $a = 0.1m^{-1}$  and the incident flux is  $G$  which is processed from the equation of the radiative transfer. when  $a \rightarrow 0, \overline{q}_r \rightarrow 0$ .

### 2.3.2. Combustion model

In this research, the probability density function (pdf) was employed to evaluate some combustion properties. Obtained from the mixture fraction to provide the effect of the turbulence fluctuation on the quantities of the conserved scalar, two types of probability density function: a clipped Gaussian and a beta function. In the present research, a beta function commonly is used for simplicity and lower cost. Beta function mathematically identified :

$$p(f) = \frac{f^{\psi-1} (1-f)^{B-1}}{\int_0^1 f^{\psi-1} (1-f)^{B-1} df} \quad (30)$$

$$f = \frac{z_i - z_{i,ox}}{z_{i,fuel} - z_{i,ox}} \quad (31)$$

explicit functions of  $(\tilde{f}, g)$  mathematically described :

$$\psi = \tilde{f} \left[ \frac{\tilde{f}(1-\tilde{f})}{g} - 1 \right] \tag{32}$$

$$B = (1 - \tilde{f})\psi \tag{33}$$

Species concentration of each product temperature and enthalpy were obtained by weighting the amount of these quantities depending (pdf) on mixture fraction,  $\tilde{p}(f)$ .  $\tilde{f}, g$  is calculated using the finite difference method for each grid,  $Q$  may be expressed, where  $\tilde{Q}$  is the Favre-averaging quantity

$$\tilde{Q} = \int_0^1 \tilde{p}(f) Q(f) df \tag{34}$$

where a mixture fraction is  $f$ , the Mean mixture fraction of mass is  $\tilde{f}$  coefficients of beta pdf are  $B, \psi$ , the mass fraction for species element  $I$  am  $Z_i$ , the mass fraction for the fuel stream inlet is  $Z_{i,fuel}$ , and the mass fraction for the oxidizer stream inlet is  $Z_{i,ox}$ .

### 3. Numerical method

The computational domain in the present work was a combustor 360× 460 mm shown in Fig. 1 in which a C2H5OH/air coaxial diffusion flame can be generated at a pressure of 2 MPa atm [19]. Combustor geometry is shown in Fig. 2. The optimal grid size of the cells is 83200×167304× 84105 and a quadrilateral refinement shape is implemented. The numerical conditions that were used are summarized in Table 1. As mentioned in the introductory part, the probability density function (PDF) is coupled with the Large Eddy Simulation (LES) and RANS turbulence model which is representing the standard k-ε turbulence model. For temporal terms, the SIMPLE algorithm as a numerical procedure with a second-order implicit scheme is adopted. For momentum, the second-order upwind is used. For boundary conditions, the inlet velocity of the droplet and the injection angle is implemented according to the experiment[22]. Fig. 3. Shows the comparison between numerical simulation using FLUENT ANSYS and the measurement.

**Table 1.** Numerical test conditions[19] [23]

parameters	units	
Atomization pressure	Mpa	2
Ethanol flow rate	g/s	0.47
Spray angle	°	45
computation domain	mm <sup>2</sup>	450×360
Velocity of inlet air through co-flow	m/s	0.32
The time step of LES/PDF	s	1× 10 <sup>-6</sup>

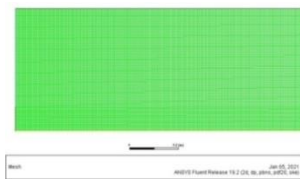


**Figure 1.** The computational domain.

### 4. Results and discussions

The injection conditions of C2H5OH/air spray combustion are used for validation related to the measurement data taken [19]. The numerical simulation for the spray combustion using RANS and LES turbulence models.

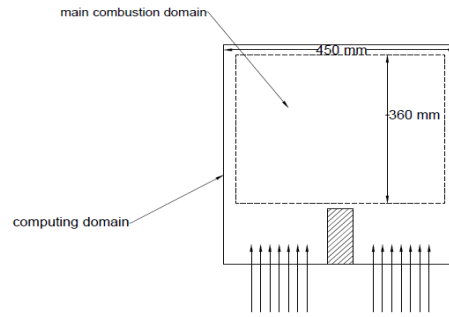


**Figure 2.** The spray combustor.

Fig. 3 shows the gas-phase temperature profiles at different levels above the nozzle at  $x = 6$  mm,  $x = 10$  mm,  $x = 20$  mm, and  $x = 25$  mm. The measurement is expressed by symbols utilizing multi-line imaging NO-LIF [13]. The dash lines demonstrate the numerical results of (the RANS) model which is representing the standard k-ε turbulence model coupled with the PDF combustion model. The solid line indicates the numerical results of large eddy simulation (LES) coupled with the PDF method. The LES/PDF gives an extremely better agreement than RANS/PDF approach. The spray flame wings are predicted by the LES/PDF approach especially at 20 mm and 25 mm better than RANS/PDF approach. According to the outcomes of the experiments, the gradients of the temperature at the flame edge are very high. This phenomenon at section 6 mm is closely predicted by the LES/PDF approach, which shows a smoother accuracy in various points of the experimental data although it predicts the gas-phase temperature at the tip edge of the nozzle is broader than the measurement data. It is important to improve the sub-grid scale combustion model for large-eddy simulation of two phases[16]while RANS/PDF in comparison with LES/PDF succeeded in predicting the regions at the tip edge of the nozzle and then the accuracy of the numerical results decreases. In section 10 mm, the numerical results predicted by LES/PDF fail in comparison with RANS/PDF approach.

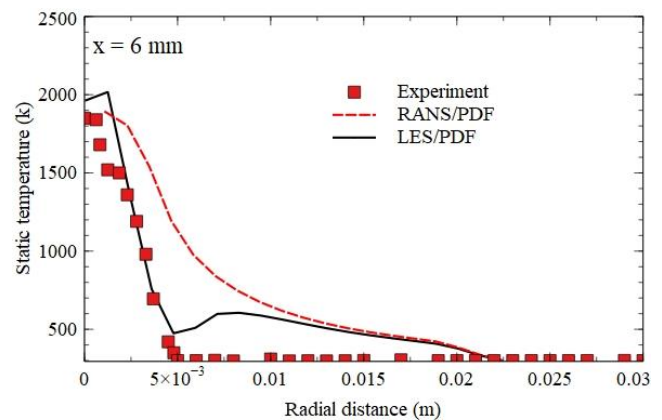
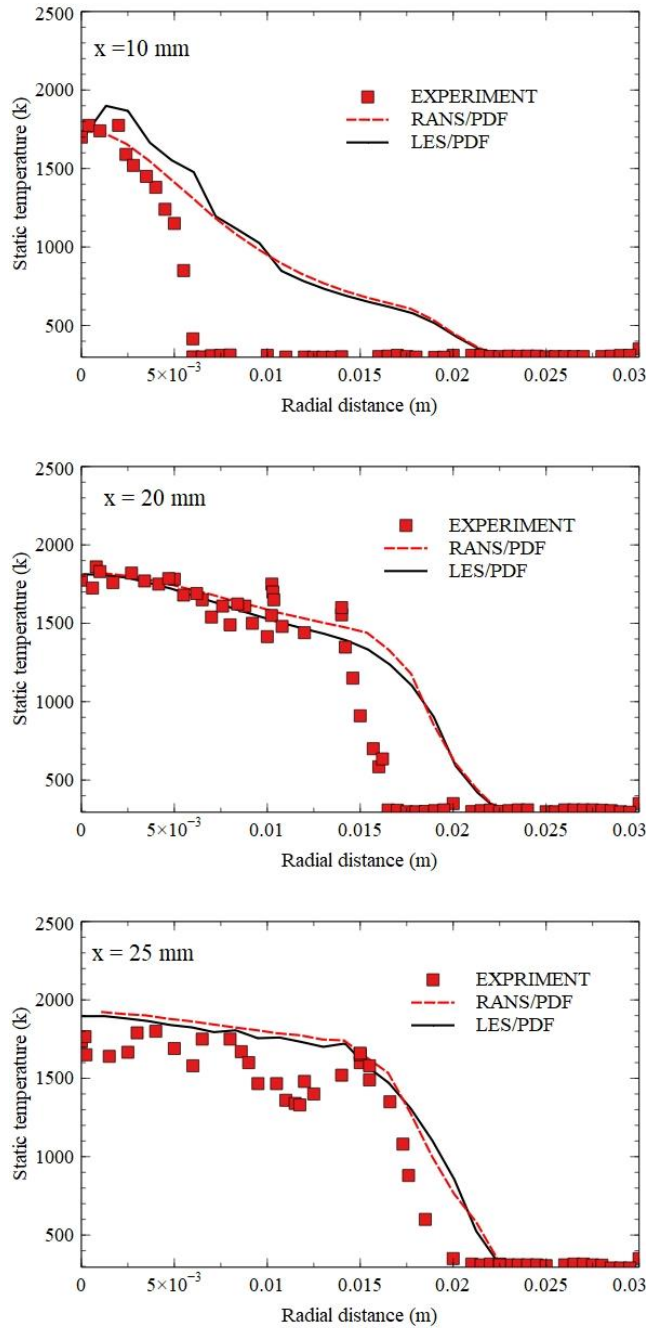


Fig. 4 demonstrates the gas phase contours of the numerical simulations that were performed by other authors in comparison with the numerical results of the present work. The difference in flame capturing is attributed to many causes such as mesh type, mesh size, numerical method procedure, approach performance, and anticipating the missing conditions. Fig. 5 shows the static temperature profiles of the present work and other authors with the experimental data at  $x=6$  mm above the nozzle. Fig. 6 shows a

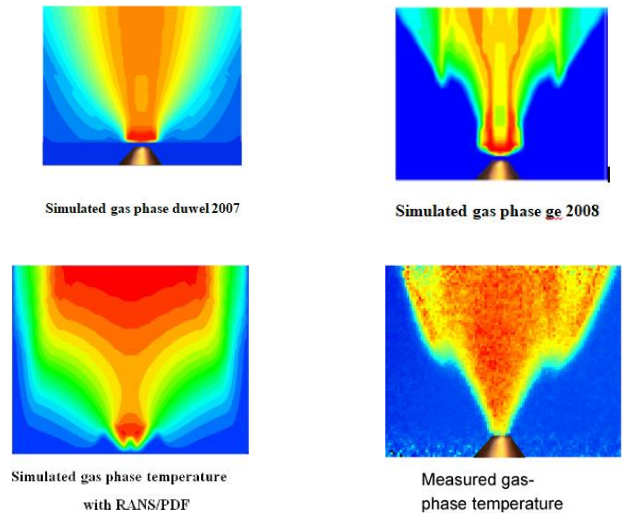
comparison of the reactions zone calculated by the experiment [14] as shown in (a), and the numerical simulation achieved using FLUENT ANSYS 19.2 in (b,c).



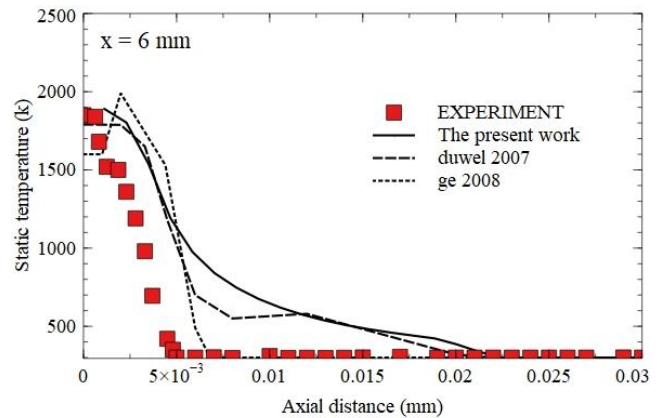
**Figure 3.** The gas-phase temperature is at different levels when  $x$  is above the exit nozzle.

Fig. 7 shows the contours of gas-phase temperature profiles. The coherent structure appears on the right side with LES/PDF which shows the eddy size and energy variation through the domain that can be explained to sub-grid scale energy equation model the ability in reinforces the prediction of

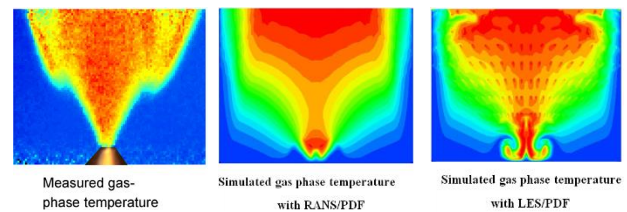
the small eddies in addition to large eddies which predict by the type of mesh utilizing in comparison to RANS/PDF approach.



**Figure 4.** Contours plot of simulated gas-phase temperature using RANS/PDF, another published work, and Spray flame photograph [19],[23].



**Figure 5.** The gas-phase temperature in comparison with another published work when  $x$  above nozzle at 6 mm [19],[23].



(a) (b) (c)  
**Figure 6.** Contours plot of simulated gas-phase temperature and Spray flame photograph [19].

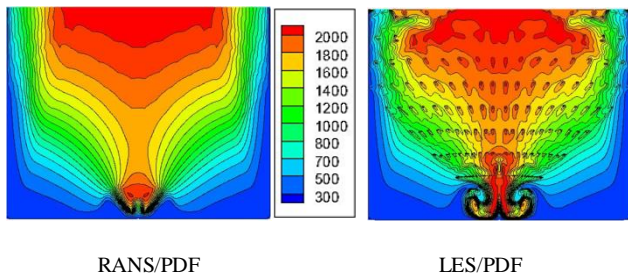


**Figure 7.** Contours plot of the gas-phase temperature at RANS turbulence model and LES.

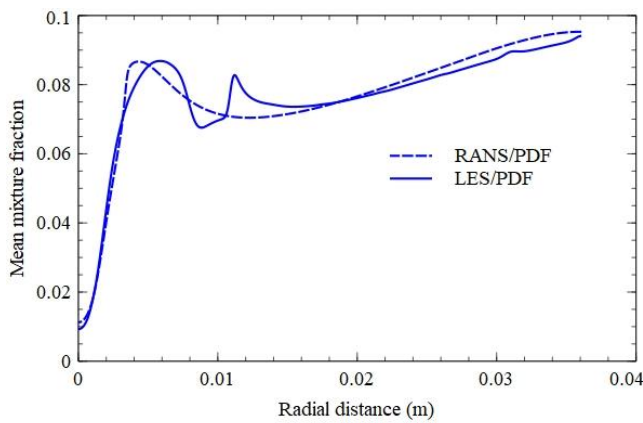
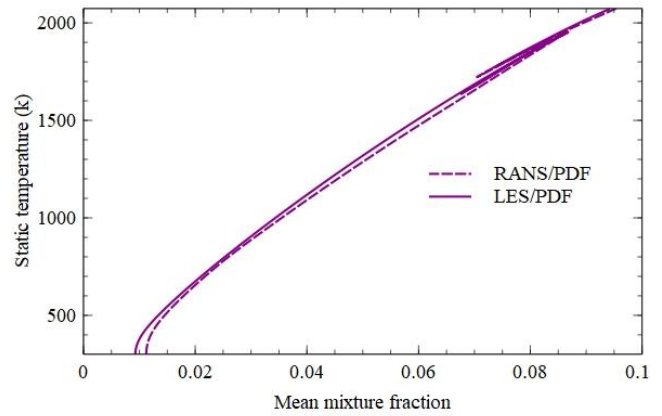


**Figure 8.** Mean mixture fraction profiles of reaction zone along with the radial distance.

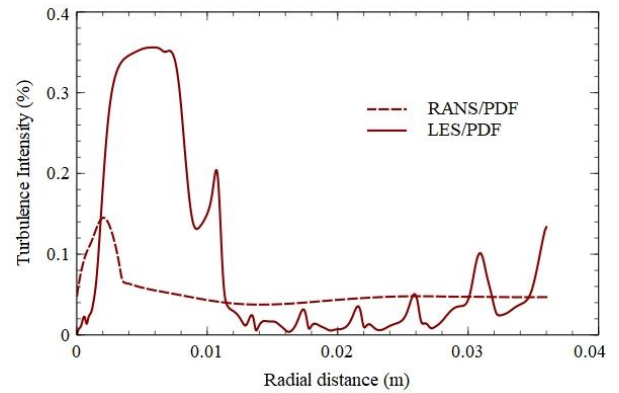
Fig. 8 shows a rising in a mean mixture fraction that can be expressed due to the evaporation rate. Mixing is relatively higher and the amount of the injected fuel at the nozzle region is higher too in comparison to the oxidizer in this domain. LES/PDF approach shows an additional consumption in fuel in comparison with RANS/PDF. Fig. 9 shows a gas temperature phase against the mean mixture fraction. There is a low distribution of mean mixture fraction (pdf) confront with the low temperature at the nozzle region and then demonstrates both static temperature and mean mixture fraction rise along with radial distance, especially in the reaction zones when the mixing is done between the ethanol stream and the oxidizer in which the burnt gas created in the upstream and blended with unburnt gas that is resulting in the generation of the high-temperature zone. In comparison, the gas temperature against pdf that is determined by using the LES/PDF approach is slightly higher than predicted by RANS/PDF approach.

Fig. 10 shows the turbulence intensity of gas-phase profiles. At the nozzle region, the turbulence intensity records a high percentage which may be expressed to the turbulence resulting from the hydrodynamic effect, the chemical interaction between two phases, liquid velocity, and the rate of evaporation, then it is eliminated with progressing away from the nozzle region. LES/PDF approach with sub-grid scale energy equation shows an additional fluctuation in the turbulence intensity profiles along with the

radial distance of the domain which demonstrates the realistic prediction in comparison with the RANS/PDF approach.



**Figure 9.** Comparison of predicted gas-phase temperature against mean mixture profiles along with the radial distance.



**Figure 10.** Comparison of predicted turbulence intensity profiles along with the radial distance.

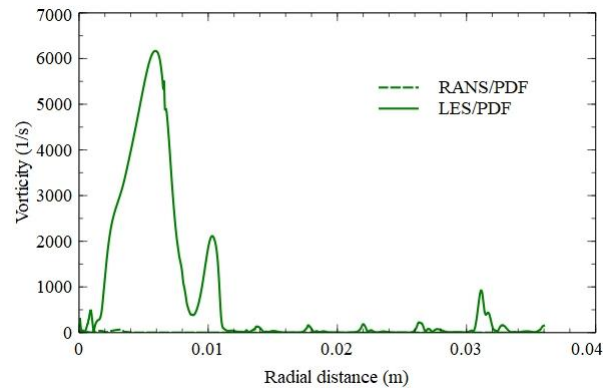


**Figure 11.** Comparison of predicted vortices profiles along with the radial distance.

Fig. 11 shows the vortices profiles along with the radial distance. In the near and inlet shear stress of the fuel jet flow, the coherent structures are expected to demonstrate and then are concentrated to be large vortices and eventually are weakly in the downstream area that can be predicted by using the LES/PDF approach while RANS/PDF approach fails in demonstration these phenomena.

#### 4. Conclusions

The turbulent spray flame of ethanol/air is studied in this work using two approaches: Large-eddy simulation coupled with a probability density function (LES/PDF) approach and standard  $k-\epsilon$  turbulence model combined with a probability density function as a combustion model (RANS/PDF) approach. Generally, the statistical results presented that are validated using the LES/PDF approach, show good agreement when compared to the experimental data and are better than those acquired by RANS/PDF approach, especially in estimating the turbulence intensity profile and vortices.

#### Authors' contribution

All authors contributed equally to the preparation of this article.

#### Declaration of competing interest

The authors declare no conflicts of interest.

#### Funding source

This study didn't receive any specific funds.

#### REFERENCES

- [1] S. Pascaud, M. Boileau, B. Cuenot, T. Poinso, Large eddy simulation of turbulent spray combustion in aeronautical gas turbines, in ECCOMAS Thematic Conference on computational combustion, 2005, pp. 149-167.
- [2] X. Jiang, G. Siamas, K. Jagus, T. Karayiannis, Physical modeling and advanced simulations of gas-liquid two-phase jet flows in atomization and sprays, *Progress in energy and combustion science*, 36(2) (2010) 131-167.
- [3] E. Gutheil, Modeling and Simulation of Droplet and Spray Combustion, *Handbook of Combustion: Online*, (2010) 205-227.
- [4] F. Jaegle, J.-M. Senoner, M. Garcia, F. Bismes, R. Lecourt, B. Cuenot, T. Poinso, Eulerian and Lagrangian spray simulations of an aeronautical multipoint injector, *Proceedings of the Combustion Institute*, 33(2) (2011) 2099-2107.
- [5] P. Senecal, E. Pomraning, K. Richards, S. Som, Grid-convergent spray models for internal combustion engine computational fluid dynamics simulations, *Journal of Energy Resources Technology*, 136(1) (2014).
- [6] N. Tanveer, C. Mohanraj, K. Jegadeesan, S. Maruthupandiyam, Comparative studies on various turbulent models with liquid rocket nozzle through computational tool, in: *Advanced Materials Research*, Trans Tech Publ, 2014, pp. 1204-1209.
- [7] M. Chrigui, A. Masri, A. Sadiki, J. Janicka, Large eddy simulation of a polydisperse ethanol spray flame, *Flow, turbulence and combustion*, 90(4) (2013) 813-832.
- [8] N.J. Georgiadis, D.P. Rizzetta, C. Fureby, Large-eddy simulation: current capabilities, recommended practices, and future research, *AIAA journal*, 48(8) (2010) 1772-1784.
- [9] W. Jones, S. Lyra, S. Navarro-Martinez, Numerical investigation of swirling kerosene spray flames using large eddy simulation, *Combustion and Flame*, 159(4) (2012) 1539-1561.
- [10] I. Dodoulas, S. Navarro-Martinez, Large eddy simulation of premixed turbulent flames using the probability density function approach, *Flow, turbulence and combustion*, 90(3) (2013) 645-678.
- [11] C. Heye, V. Raman, A.R. Masri, LES/probability density function approach for the simulation of an ethanol spray flame, *Proceedings of the Combustion Institute*, 34(1) (2013) 1633-1641.
- [12] S. Ukai, A. Kronenburg, O. Stein, LES-CMC of a dilute acetone spray flame, *Proceedings of the Combustion Institute*, 34(1) (2013) 1643-1650.
- [13] W. Jones, A. Marquis, K. Vogiatzaki, Large-eddy simulation of spray combustion in a gas turbine combustor, *Combustion and flame*, 161(1) (2014) 222-239.
- [14] S. Ukai, A. Kronenburg, O. Stein, Large eddy simulation of dilute acetone spray flames using CMC coupled with tabulated chemistry, *Proceedings of the Combustion Institute*, 35(2) (2015) 1667-1674.
- [15] I.A. Dodoulas, S. Navarro-Martinez, Analysis of extinction in a non-premixed turbulent flame using large eddy simulation and the chemical explosion mode analysis, *Combustion Theory and Modelling*, 19(1) (2015) 107-129.
- [16] Q. Wang, T. Jaravel, M. Ihme, Assessment of spray combustion models in large-eddy simulations of a polydispersed acetone spray flame, *Proceedings of the Combustion Institute*, 37(3) (2019) 3335-3344.
- [17] F.L. Sacomano Filho, L. Dressler, A. Hosseinzadeh, A. Sadiki, G.C. Krieger Filho, Investigations of evaporative cooling and turbulence flame interaction modeling in ethanol turbulent spray combustion using tabulated chemistry, *Fluids*, 4(4) (2019) 187.
- [18] D. Paulhiac, B. Cuenot, E. Riber, L. Esclapez, S. Richard, Analysis of the spray flame structure in a lab-scale burner using large eddy simulation and discrete particle simulation, *Combustion and Flame*, 212 (2020) 25-38.
- [19] H.-W. Ge, I. Düwel, H. Kronemayer, R. Dibble, E. Gutheil, C. Schulz, J. Wolfrum, Laser-based experimental and Monte Carlo PDF numerical investigation of an ethanol/air spray flame, *Combustion science and technology*, 180(8) (2008) 1529-1547.
- [20] A. Fluent, 17.0 Theory Guide, 2015, Canonsburg, PA 15317: ANSYS, in, Inc.
- [21] S. Morsi, A. Alexander, An investigation of particle trajectories in two-phase flow systems, *Journal of Fluid mechanics*, 55(2) (1972) 193-208.
- [22] P. Lavielle, F. Lemoine, G. Lavergne, M. Lebouché, Evaporating and combusting droplet temperature measurements using two-color laser-induced fluorescence, *Experiments in fluids*, 31(1) (2001) 45-55.
- [23] I. Düwel, H.-W. Ge, H. Kronemayer, R. Dibble, E. Gutheil, C. Schulz, J. Wolfrum, Experimental and numerical characterization of a turbulent spray flame, *Proceedings of the Combustion Institute*, 31(2) (2007) 2247-2255.